Evolution of Mid-gap States and Residual 3-Dimensionality in $La_{2-x}Sr_xCuO_4$

S. Sahrakorpi[1], M. Lindroos[1,2], R.S. Markiewicz[1] and A. Bansil[1]
[1] *Physics Department, Northeastern University, Boston, Massachusetts 02115, USA*
[2] *Institute of Physics, Tampere University of Technology, P.O. Box 692, 33101 Tampere, Finland*
(Dated: February 2, 2008)

We have carried out extensive first principles doping-dependent computations of angle-resolved photoemission (ARPES) intensities in $La_{2-x}Sr_xCuO_4$ (LSCO) over a wide range of binding energies. Intercell hopping and the associated 3-dimensionality, which is usually neglected in discussing cuprate physics, is shown to play a key role in shaping the ARPES spectra. Despite the obvious importance of strong coupling effects (e.g. the presence of a lower Hubbard band coexisting with mid-gap states in the doped insulator), we show that a number of salient features of the experimental ARPES spectra are captured to a surprisingly large extent when effects of k_z-dispersion are properly included in the analysis.

PACS numbers: 79.60.-i, 71.18.+y, 74.72.Dn

$La_{2-x}Sr_xCuO_4$ (LSCO) has drawn intense interest as a model system for understanding one of the most hotly debated issues in condensed matter physics currently, namely, how does a Mott insulator, La_2CuO_4 (LCO), develop into a superconductor when doped with holes via La/Sr substitution, and what is the route taken by the electronic states in the insulator to achieve this remarkable transformation into a metal.[1,2] Angle-resolved photoemission spectroscopy (ARPES) has been brought to bear on these questions in recent years as techniques for preparing LSCO surfaces have improved.[3,4,5,6,7,8] ARPES spectra in LCO find a lower Hubbard band (LHB) associated with an insulating state, which persists with finite hole doping, losing intensity without shifting in energy. At the same time *new states* – the so-called mid-gap states – appear close to the Fermi level, which evolve into the conventional metallic bands near optimal doping. Doping-dependent ARPES spectra in LSCO thus address a wide range of issues concerning stripe and pseudogap physics and their relation to the mechanism of high-temperature superconductivity, and bear on questions of non-Fermi liquid behavior or gossamer superconductivity[9,10], among others.[11]

We have recently shown with the example of Bi2212 that the residual k_z-dispersion of bands in a quasi-2D material will induce an irreducible linewidth in ARPES peaks, which is unrelated to any scattering mechanisms.[12] This effect becomes accentuated in LSCO, where the bands possess a greater 3D character compared to Bi2212. This article reports extensive first principles computations of the ARPES intensity in LSCO with the goal of ascertaining the extent to which k_z-dispersion affects the experimental spectra of the mid-gap and LHB states. The calculations properly model the photoemission process and include the crystal wave functions to describe the initial and final states in the presence of the surface and take account of the associated dipole matrix element and its dependencies on photon energy and polarization. The interplay between the effects of the ARPES matrix element[13,14,15] and the k_z-dispersion yields computed intensity maps for emission from the Fermi energy (E_F) as well as for binding energies several hundred meV's below E_F, which are in surprising accord with the corresponding measurements.

Our calculations give insight into a number of salient features of the experimental spectra such as, the dispersion of the mid-gap states and the characteristic broadenings and symmetries or lack thereof in the photointensities. Evidence of physics beyond the framework of the conventional local density approximation (LDA) based picture is especially clear in the strongly underdoped regime, both in the appearence of a d-wave-like pseudogap in the mid-gap states and in the presence of the LHB near half filling. We discuss this insulating regime in terms of tight-binding (TB) computations, in which the LDA-inspired overlap parameters are supplemented with a Hubbard U or a pseudogap Δ. The effect of k_z-dispersion is included through an intercell hopping parameter – to our knowledge for the first time in connection with a TB description of the cuprates. In this way, via comparisons between theory and experiment, we adduce a strong connection between the LDA generated metallic states and the evolution of the mid-gap band throughout the doping range.

With regard to relevant computational details, the fully self-consistent electronic structure of tetragonal LCO was obtained within the LDA by using the well-established all electron Green function methodology[16]; our band structure and Fermi surface (FS) are in accord with published data[17]. Following common practice, the metallic state of LSCO obtained by doping LCO with Sr is assumed to be described by the LDA generated metallic band structure for LCO. The effect of La/Sr substitution is mainly to adjust the electron concentration and, therefore, we have modeled LSCO at any given x-value by invoking a rigid band filling of the band structure of LCO with the appropriate number of electrons per unit cell. All presented ARPES intensities have been computed within the one-step photoemission formalism, assuming an LaO-layer terminated surface; see Refs. 13,14 and 12 for details.

Fig. 1 considers emission from E_F for optimally doped

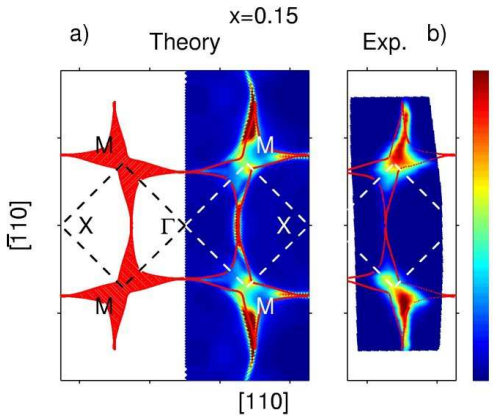

FIG. 1: (Color) ARPES spectra for emission from the Fermi energy in optimally doped LSCO for $x = 0.15$. (a): Red filled region on left hand side gives the 3D Fermi surface projected onto the (k_x, k_y)-plane, and denotes the area of allowed emissions. The right hand side gives computed intensity including the effect of the ARPES matrix elements with red lines marking boundaries of the red filled regions. (b): Corresponding experimental spectra[4].

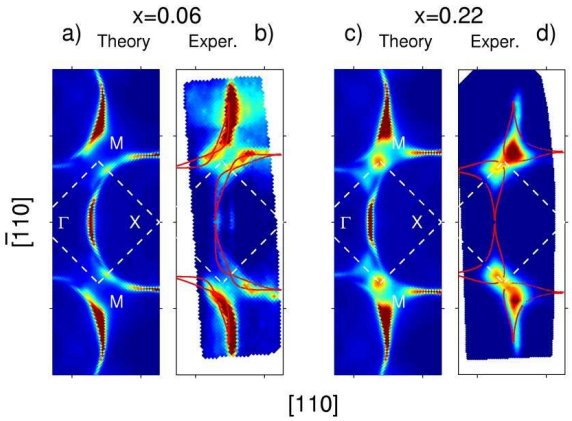

FIG. 2: (Color) Similar to Fig. 1, except that this figure compares theoretical and experimental ARPES intensities in the underdoped $x = 0.06$ [panels (a) and (b) (Ref. 8)] and overdoped $x = 0.22$ [panels (c) and (d) (Ref. 5)] cases.

LSCO and shows the remarkable degree to which the FS map can be understood within the framework of the conventional LDA-based picture. We start by looking at the left side of (a), where the filled red region gives the projection of the FS onto the (k_x, k_y)-plane and encompasses various FS cross-sections as a function of k_z.[18] Emission of photoelectrons is possible in principle from any part of this red region due to the quasi-2D nature of states. [In a strictly 2D system, the red region will collapse into a standard FS contour of zero width.] We emphasize that the photointensity within this red region will in general not be uniform as it will be modified by the effect of the ARPES matrix element. This aspect is delineated on the right side of (a), where the theoretically predicted ARPES intensity is shown superposed with the boundaries of the region of allowed transitions by red lines.

When we compare the theoretical intensities in Fig. 1(a) with the corresponding experimental results[4,19] in Fig. 1(b), the most striking feature is the appearance of wing-like structures around the anti-nodal points $M(\pi, 0)$ in both theory and experiment. On the other hand, along the nodal direction in the first Brillouin zone (BZ), Γ to $X(\pi, \pi)$, the high computed intensity is not reproduced in the measurements. However, we find that this computed nodal intensity is quite sensitive to photon energy. It will be necessary to carry out ARPES experiments over a range of photon energies in order to ascertain whether or not absence of nodal intensity represents a significant effect of correlations beyond the LDA in LSCO.

Figure 2 expands the preceding discussion to include the underdoped and overdoped regimes. The computations in all cases simulate experimental conditions[5,8] of resolution, polarization of light and photon energy. The theory is seen to provide a good overall description of the data over the entire doping range, discrepancies along the nodal direction notwithstanding. Around the antinodal point, incorporation of k_z-dispersion allows the evolution of the FS across the (broadened) Van Hove singularity (VHS) to be analyzed in detail. In the underdoped sample the intensity is concentrated in two features lying above and below the $M(\pi, 0)$-point. In contrast, the FS crosses the VHS near optimal doping, and the overdoped sample displays a greater spectral weight around the $M(\pi, 0)$-point. Since the midgap states evolve into conventional bands with increased doping, the good agreement with theory is perhaps to be expected in optimally and overdoped samples, but the continued agreement for the underdoped sample is quite remarkable – particularly since the midgap states have a pseudogap, as discussed below.

Figs. 1 and 2 make it clear that the broadening of ARPES spectra resulting from the effect of k_z-dispersion is essentially zero along the nodal direction and that it increases only gradually as one moves towards the antinodal region. By contrast in the antinodal region, the effects of the VHS conspire with those of the k_z-dispersion to produce effective linewidths which increase rapidly as one moves away from the antinodal point. The antinodal point itself is anomalous in that the broadening can be quite small parallel to the BZ boundary ($X(\pi, \pi)$ to $M(\pi, 0)$) as seen for example from Fig. 2(a). The present analysis shows that, even if correlation effects were absent, features in the antinodal region would generally be considerably broader than nodal ones, due simply to the effect of k_z-dispersion.

Caution should be exercised in interpreting the significance of differences between theory and experiment in Figs. 1 and 2 around say the $M(\pi, 0)$-point or for that matter even the nodal direction. On the theoretical side, some of these details are sensitive to photon energy and to the precise position of the Fermi energy in relation to the VHS in the density of states. Similarly,

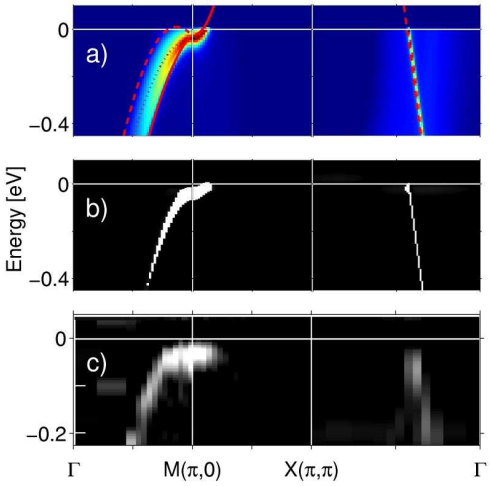

FIG. 3: (Color) Band dispersion in optimally doped LSCO, $x = 0.15$. (a): Computed ARPES intensities along the $\Gamma - M - X - \Gamma$ -line in the BZ; color scale is the same as that in Fig. 1. Red lines give bands corresponding to different values of k_z: $k_z = 0$ (solid line), $k_z = \pi/c$ (dotted), and $k_z = 2\pi/c$ (dashed). (b): Second derivative of the theoretical spectra in (a) as a grey scale plot. (c): Experimental second derivatives[6] corresponding to the theoretical results in (b). Note scale change between panels (b) and (c).

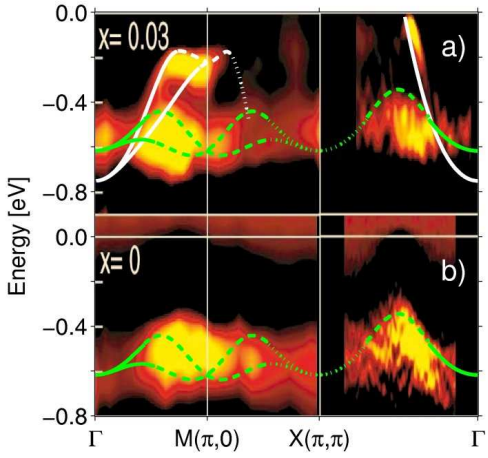

FIG. 4: (Color) Theoretical band structures of LSCO are shown overlayed on experimental ARPES spectra (second derivatives) of Ref. 7 for two different dopings: (a) $x = 0.03$, and (b) $x = 0.0$. The data are given on a hot color scale in which red and black denote lows. Two sets of tight-binding bands are shown by green and white lines as detailed in the text. The two different bands in each case correspond to two values of k_z: $k_z = 0$ and $k_z = 2\pi/c$. Different line types denote computed relative spectral weights varying from 1.0-0.8 (solid lines), 0.8-0.2 (dashed) and 0.2-0.01 (dotted).

higher resolution experiments are needed to pin down some of the fine details in the experimental spectra.[20] Ultimately, ARPES evidence for exotic physical effects beyond the conventional LDA-type pictures (e.g. stripes, pseudogaps, strong correlations) must derive from a careful analysis of the differences in the fine structure between theoretical and experimental intensities such as those of Figs. 1 and 2.

The typical behavior of spectra below E_F is considered in Fig. 3 with the example of the optimally doped system. Much of the commentary in connection with Figs. 1 and 2 above is applicable and need not be repeated. In Fig. 3(a), the computed ARPES intensity along the $\Gamma - M$ as well as the $\Gamma - X$-directions lies within the limits given by the bands for various k_z-values, albeit with a strong modulation by the ARPES matrix element. Once again, the spectral lines are substantially broader along $\Gamma - M$ compared to $\Gamma - X$. Theoretical and experimental[6] results in (b) and (c), respectively, are in substantial accord in this respect. Note differences in vertical scale in (b) and (c), indicating a renormalization (i.e. reduction) in bandwidth by roughly a factor of two over the LDA predictions, which is quite common in the cuprates. Also, the measured ARPES intensity in (c) is seen to pull away from the Fermi energy, which is not the case in the theoretical plot of (b). This difference however is to be expected since the theory refers to the normal state, while the measurements are taken from a superconducting sample.

We have fitted the first principles FS and band dispersions near E_F in LSCO within the TB model using the form[12]

$$\epsilon_k = -2t(c_x + c_y) - 4t' c_x c_y - 2t''(c_{2x} + c_{2y}) \\ -2\,T_z(\vec{k}_\parallel)\, c_z (c_x - c_y)^2, \qquad (1)$$

with $c_i = cos(k_i a)$ and $c_{2i} = cos(2k_i a)$, $i = x, y$, $c_z = cos(k_z c/2)$, and

$$T_z = t_z\, cos(k_x a/2)\, cos(k_y a/2). \qquad (2)$$

The extra angular dependence in Eq. 2 accounts for the staggered stacking of neighboring CuO_2-planes, and results in vanishing k_z-dispersion along the BZ boundaries. The parameters which yield a good fit are: $t = 0.32eV$, $t' = -0.25t$, $t'' = -0.02t$, and $t_z = 0.16t$. The latter value should be compared with $t_z = 0.11t$ estimated from transport.[21] In order to simulate the presence of a pseudogap and/or the superconducting gap, the bare bands of Eq. 1 should be replaced by: $\epsilon_k \to \pm E_k$, where $E_k^2 = \epsilon_k^2 + \Delta_k^2$ and $\Delta_k = \Delta_0(c_x - c_y)/2$. In this way a d-wave-like gap with a maximum value of Δ_0 at the $M(\pi, 0)$-point is produced in the spectrum; we find that Δ_0 grows with underdoping as a pseudogap.

Fig. 4 considers the underdoped regime below the superconductor-insulator (SI) transition (around $x = 0.06$). Focusing on the experimental[7] spectra first, the half-filled case ($x = 0.0$) in (b) is seen to display the presence of the lower Hubbard band (LHB) at a binding energy of ≈ 0.5 eV, and little weight around E_F. When the system is doped with a small amount of holes, we see from (a) the appearance of a substantial weight in

the mid-gap spectrum near the $M(\pi,0)$ and $(\pi/2,\pi/2)$ points, while the LHB is essentially unchanged.

The experimental results of Fig. 4 cannot of course be understood within the conventional LDA-based picture, which fails to produce the insulating state at half-filling. Insight can however be obtained via the TB model, and accordingly, we have carried out two sets of such calculations: (i) The LHB is fit to TB mean-field computations for a saturated antiferromagnet with Hubbard parameter $U = 6t$, with all other parameters taken directly from the LDA bands. The k_z-dispersion is accounted for via the t_z parameter (see Eqs. 1 and 2), which to our knowledge has not been included in any previously published work. These TB bands for the two extremal k_z-values are given by green lines in Fig. 4, with different line types giving associated spectral weights (see figure caption). Our parameter values are consistent with earlier data from insulating cuprates based on the ARPES[22] and spin wave spectra[23]. (ii) TB calculations with the same parameters as those used in the preceding case, except that the Hubbard parameter U is replaced by a d-wave-like pseudogap with $\Delta_0 = 220$ meV at $M(\pi,0)$, which accounts for the presence of such a gap in the experimental spectra at $x = 0.03$.

The theoretical bands of Fig. 4 provide a handle on understanding some salient features of the experimental spectra. We consider the LHB along the $\Gamma - M$ and $M - X$ lines first. At both $x = 0$ and $x = 0.03$, the measured LHB is seen to extend over the binding energy range of 0.4-0.8 eV, more or less symmetrically about the $M(\pi,0)$-point, at least insofar as its width is concerned. Much of this width can be ascribed to the effect of k_z-dispersion, which will induce spectral lines to spread between the boundaries given by the pair of green bands. Note also that the computed LHB is symmetric around $M(\pi,0)$ due to the effect of zone-folding in the AFM insulating state. The calculated spectral weights of the green bands are seen to be larger along $\Gamma - M$ compared to the $M - X$ line.[24] The experimental broadening at $M(\pi,0)$ is anomalously large and not due to k_z-dispersion. This however is not surprising since the $M(\pi,0)$-point lies on the AFM zone boundary and is susceptible to 'hot spot' scattering. The situation along the $\Gamma - X$ line is sharply different. Here the effect of k_z-dispersion is negligible. Moreover, $\Gamma - X$ is orthogonal to the AFM zone boundary. Therefore, substantial observed widths of the LHB along $\Gamma - X$ cannot be due to the effect of either k_z-dispersion or of magnetic scattering.

We turn now to comment on the mid-gap spectrum in Fig. 4(a). Here the aforementioned symmetry of the LHB with respect to the $M(\pi,0)$-point is absent. The intensity of mid-gap states cuts off quite abruptly near the M-point along the $M-X$ line. This is in accord with the LDA-based bands (white lines), which show little effect of k_z-dispersion and also possess little weight to the right hand side of $M(\pi,0)$. On the other hand, a broad patch of intensity is seen around $M(\pi,0)$ extending toward Γ. This is to be expected due to the effect of k_z-dispersion in view of the boundaries given by the pair of white LDA-based bands.[24] Interestingly, along the $\Gamma - X$ -line, the experimental mid-gap band is quite sharply defined, consistent with the fact that the LDA bands display little k_z induced broadening.

Taken together, the comparisons of Figs. 1-4 paint a remarkable picture of the way mid-gap states evolve in LSCO with doping. The fact that the spectrum of the lightly doped insulator along the $\Gamma - X$ line in Fig. 4(a) essentially follows the LDA bands, suggests that even the first mid-gap states created when holes are added into the Mott insulator mimic metallic states.[25] However, the precise nature of the mid-gap states and how the associated pseudogap evolves to yield a Luttinger-like Fermi surface remains an important theoretical question. The fact that hopping appears only weakly renormalized with doping, but that the spectral weight or the intensity of the mid-gap band scales with x, is much in the spirit of a gossamer type model[9,10]. The presence of a pseudogap near $(\pi,0)$ will result in predominantly incoherent c-axis transport in the underdoped cuprates[26], whereas there may be coherent c-axis transport in overdoped samples.[27] Certainly, the ARPES spectra in the vicinity of E_F are described in considerable detail by the LDA computations as seen from Figs. 1 and 2.

In conclusion, we have shown with the example of LSCO, that effects of k_z-dispersion, which have been neglected in most of the existing literature on the cuprates, play a key role in explaining the observed broadening in the ARPES spectra throughout the BZ for both the mid-gap band as well as the LHB. These results provide a new benchmark for testing strong correlation models of the ARPES spectra. For example, evidence for stripe or marginal Fermi liquid physics[28] must take into account the ω-dependent broadening associated with k_z-dispersion. Finally, despite the obvious importance of strong correlation effects, the remarkable extent to which simple LDA-type metallic states describe the dispersion of the mid-gap spectrum in LSCO is an observation calling for theoretical interpretation. Our results will provide a deeper understanding of strong correlation effects in the cuprates, including insight into the mid-gap states and the pseudogap, and will likely require some revisions of associated models.

Acknowledgments

This work is supported by the US Department of Energy contract DE-AC03-76SF00098, and benefited from the allocation of supercomputer time at NERSC, Northeastern University's Advanced Scientific Computation Center (ASCC), and the Institute of Advanced Computing (IAC), Tampere.

[1] J. Orenstein and A.J. Millis, Science **288**, 468 (2000).
[2] M. Greiner, et al., Nature **415**, 39 (2002).
[3] X.J. Zhou, et al., Science **286**, 268 (1999).
[4] X.J. Zhou, et al., Phys. Rev. Lett. **86**, 5578 (2001).
[5] T. Yoshida, et al., Phys. Rev. B **63**, 220501(R) (2001).
[6] A. Ino, et al., Phys. Rev. B **65**, 094504 (2002).
[7] T. Yoshida, et al., Phys. Rev. Lett. **91**, 027001 (2003).
[8] X.J. Zhou, et al., Phys. Rev. Lett. **92**, 187001 (2004).
[9] R.B. Laughlin, cond-mat/0209269 (unpublished).
[10] F.C. Zhang, Phys. Rev. Lett. **90**, 207002 (2003).
[11] A. Damascelli, et al., Rev. Mod. Phys. **75**, 473 (2003).
[12] A. Bansil, et al., Phys. Rev. B **71**, 012503 (2005).
[13] A. Bansil and M. Lindroos, Phys. Rev. Lett. **83**, 5154 (1999).
[14] M. Lindroos, et al., Phys. Rev. B **65**, 054514 (2002).
[15] S. Sahrakorpi, et al., Phys. Rev. B **68**, 054522 (2003).
[16] See, e.g., A. Bansil, et al., Phys. Rev. B **60**, 13396 (1999), and references therein.
[17] J. Yu, et al., Phys. Rev. Lett. **58**, 1035 (1987).
[18] Following the experimental setup of integrating over narrow energy window, the projected FS's in Figs. 1 and 2 are integrated over relevant energy windows as follows: For $x = 0.06$, $E_F \pm 5meV$; For $x = 0.15, 0.22$, $E_F - 30meV + 5meV$.
[19] We thank X.J. Zhou, T. Yoshida, A. Fujimori, Z. Hussain, and Z.X. Shen, for providing us with the original experimental data of Figs. 1 and 2.
[20] Note, for example, that the experimental spectra in Figs. 1(b), 2(b) and 2(d) are not completely symmetric with respect to the the upper and lower M-points.
[21] R.S. Markiewicz, Phys. Rev. B **70**, 174518 (2004).
[22] C. Kusko, et al., Phys. Rev. B **66**, 140513(R) (2002).
[23] N.M.R. Peres and M.A.N. Araújo, Phys. Stat. Sol. **236**, 523 (2003).
[24] There will of course be additional modulation of the spectra due to the ARPES matrix element, which has not been included in the TB computations of Fig. 4.
[25] ARPES studies of $Ca_2CuO_2Cl_2$ (CCOC) reveal a similar situation, i.e., the presence of a LHB which evolves weakly with doping, while near the FS mid-gap states appear which resemble the bare bands [K.M. Shen, et al., Phys. Rev. Lett. **93**, 267002 (2004)].
[26] J.H. Kim, et al., Physica C **247**, 297 (1995).
[27] Notably, coherent 3D coupling has been reported recently in an overdoped Tl-cuprate by N.E. Hussey, et al., Nature **425**, 814 (2003).
[28] T. Valla, et al., Nature **417**, 627 (2002).